Excitation of Rydberg wave packets in the tunneling regime

B. Piraux[1a], F. Mota-Furtado[2], P. F. O'Mahony[2],
A. Galstyan[1] and Yu. V. Popov[3,4]
[1] *Institute of Condensed Matter and Nanosciences, Université Catholique de Louvain, 2 chemin du cyclotron, Box L7.01.07, B-1348 Louvain-la-Neuve, Belgium*
[2] *Department of Maths, Royal Holloway, University of London, Egham, Surrey TW20 0EX, United Kingdom*
[3] *Skobeltsyn Institute of Nuclear Physics, Moscow State University, Moscow, Russia*
[4] *Joint Institute for Nuclear Research, Dubna, Russia*

In the tunneling regime for strong laser field ionization of atoms, experimental studies have shown that a substantial fraction of atoms survive the laser pulse in many Rydberg states. To explain the origin of such trapping of population into Rydberg states, two mechanisms have been proposed : the first involves AC-Stark-shifted multiphoton resonances and the second, called frustrated tunneling ionization, leads to the recombination of tunneled electrons into Rydberg states. We use a very accurate spectral method based on complex sturmian functions to solve the time dependent Schrödinger equation for hydrogen in a linearly polarized infrared pulse and to calculate the tunneling probability in terms of the atomic ground state width. We examine the probability of excitation into Rydberg states as a function of the peak intensity for various pulse durations and two wavelengths, 800 nm and 1800 nm and try to explain the results in light of the two aforementioned mechanisms. For long pulses of 800 nm wavelength, the extreme sensitivity of the trapping of population into high-lying Rydberg states to the peak intensity, the well defined value and parity of the angular momentum of the populated Rydberg states and the presence of Freeman resonances can be explained using a multiphotonic excitation mechanism. For strong pulses of 1800 nm wavelength, in the so-called adiabatic or quasi-static tunneling regime, the oscillations of the excitation probability as a function of intensity are in phase opposition to the ionization probability and we observe a migration towards high values of the angular momentum with different distributions in the angular momentum at the maxima and minima of the oscillations. We also present a detailed study of how the excited state wave packet builds up in time during the interaction of the atom with the pulse.

PACS numbers: 32.80.Fb, 31.30.jn

a. bernard.piraux@uclouvain.be

I. INTRODUCTION

Keldysh theory [1] has laid the foundation of our understanding of the ionization of atoms and molecules by strong laser fields. For weak fields, ionization results from a multiphoton process while for field strengths comparable to the Coulomb binding force, ionization takes place predominantly by tunneling. The study of tunnel ionization has led to an enormous amount of theoretical and experimental work, resulting in several breakthroughs within the new field of attosecond physics [2]. By contrast, the study of excitation of Rydberg wave packets in the regime of tunnel ionization has attracted much less attention because of the difficulties it poses both from experimental and theoretical points of view. In this contribution, we wish to shed some light on the mechanisms leading to the excitation of Rydberg wave packets in the tunneling regime of ionization.

In their experiment on He at a wavelength of 800 nm, Nubbemeyer *et al.* [3] observed a substantial fraction of neutral atoms surviving the laser pulse in excited states for a broad range of field intensities up to 10^{15} W/cm^2. In addition, they showed that the probability of excitation decreases rapidly with increasing laser ellipticity. As their findings are compatible with the strong field tunneling-plus-rescattering model, they concluded that the excited state population trapping is predominantly due to a recombination process that they called frustrated tunneling. Very high-lying Rydberg states with principal quantum number $n \approx 100$ have also been detected very recently in Ar at 800 nm in a coincidence spectroscopy experiment by Larimian *et al.* [4]. Although this latter experiment was performed at much lower peak intensity, not in the deep tunneling regime, they also interpreted the creation of very high-lying Rydberg states in terms of frustrated tunneling. By contrast, in an earlier experiment on Kr and Xe at a wavelength of 770 nm and a peak intensity of 5×10^{15} W/cm^2, Jones *et al.* [5] observed significant population trapping into Rydberg states, which was explained in terms of AC-Stark-shifted resonances.

Evidence for the underlying dynamics of trapping of population in excited states can also be extracted indirectly from the study of harmonic generation spectra. Various experiments in Ar at 800 nm wavelength show that resonance enhancement occurs for high order harmonics near the ionization threshold for relatively low peak intensities of the laser pulse. This indicates that multiphoton processes leading to trapping of population in many excited states, play an important role in the dynamics. In the earliest of these experiments, Toma *et al.* [6] showed that for a long (140 fs) pulse with a flat-top intensity profile, the signal of the 13th harmonic, which is two photons above the ionization threshold, is strongly enhanced. Chini *et al.* [7] studied the spatial distribution of the 9th harmonic, just below the ionization threshold. At a relatively low peak intensity (about 2×10^{13} W/cm^2) and near the atomic resonance, they observe a significant enhancement of this harmonic, leading to spatially coherent VUV emission with a high conversion efficiency. Recently, Beaulieu *et al.* [8] studied the spectral, spatial and temporal characteristics of the radiation produced near the ionization threshold of Ar by few-cycle laser pulses. They showed that multiple infrared photons are absorbed to populate excited states. This, in turn, leads either to direct extreme ultraviolet emission through free induction decay or to the generation of high-order harmonics through ionization from these states and recombination to the ground state.

From the theoretical point of view, a careful examination of the trapping of population into Rydberg states requires an accurate solution of the time-dependent Schrödinger equation (TDSE) whilst allowing for the population of high lying Rydberg states. This is not an easy task even in the case of atomic hydrogen. A first attempt has been made by Li *et al.* [9, 10]. They claimed that population trapping into Rydberg states can be understood in terms of multiphotonic transitions from the ground state rather than by frustrated tunneling. Recently, Zimmermann *et al.* [11] claimed that the interpretation of population trapping into Rydberg states in terms of frustrated tunneling is complementary to the multiphoton picture while providing a time dependent perspective on the excitation process.

Frustrated tunneling designates a process in which Rydberg states are populated when tunneled electrons that do not gain sufficient energy from the laser pulse are captured by the Coulomb field. The capture of a tunneled electron into a Rydberg state can occur when, driven by the field, this electron returns to the parent ion. However, as shown by Liu *et al.* [12], a tunneled electron emitted in the transverse direction can also be trapped into a Rydberg orbit. The theoretical treatment of frustrated tunneling is based on the two-step semiclassical model including the tunnel ionization step followed by a classical propagation.

To address the possible mechanisms for excitation of Rydberg states we consider the interaction of atomic hydrogen with strong, linearly polarized, low-frequency radiation pulses. We solve the TDSE by means of a spectral method in which the total wave function is expanded in a basis of complex Coulomb sturmian functions that are known to describe very accurately the bound spectrum of atomic hydrogen. In addition, we use this spectral method to calculate the ionization probability in the static field limit. Our calculations focus on two parameter regions : the

non-adiabatic and the adiabatic or quasi-static tunneling regimes which are briefly described in the second section of this contribution. In the third section, we calculate the probability of excitation as a function of the peak intensity for various pulse durations and two wavelengths, 800 nm and 1800 nm. We analyze the compatibility of our results with both a recombination mechanism and a multiphotonic process. In the final section, we study how the Rydberg wave packet builds up in time during the interaction of the atom with the pulse before concluding.

Atomic units ($\hbar = e = m_e = 1$) are used throughout unless otherwise specified.

II. THEORETICAL CONSIDERATIONS

When an atom interacts with an intense, linearly polarized electric field of very low frequency, Keldysh [1] in his 1965 seminal paper showed that the atom, assumed initially in its ground state, ionizes through a tunneling process. He introduced the so-called adiabaticity parameter $\gamma = \omega\sqrt{2I_p}/E$ where ω is the photon energy, I_p the ionization potential and E the electric field amplitude. For $\gamma \ll 1$, ionization occurs predominantly through a quasi static tunneling process. It corresponds to the adiabatic limit, where for a fixed peak intensity, the field frequency $\omega \to 0$ while keeping the number N of optical cycles within the pulse constant. In this limit, the tunneling probability is given by :

$$P_{\rm ion} = 1 - \exp\left\{-\frac{1}{\omega}\int_{-N\pi}^{N\pi} d\tau\ \Gamma_g\left(|E(\tau)|\right)\right\}, \tag{1}$$

where $\tau = \omega t$. In this expression, Γ_g is the width of the atomic ground state in a static field, which is calculated as a function of the instantaneous electric field $E(\tau)$ using complex scaling. Note that, the exponential term represents the probability to stay in the ground state. It means that in this limit, the excitation probability tends to zero. The range of intermediate $\gamma \sim 1$, which is typical for many current intense field experiments, is the regime of non adiabatic tunneling [13]. Finally, for $\gamma > 1$, ionization occurs through a multiphoton process.

To study the ionization and excitation yields in these various regimes, we consider the case of atomic hydrogen, in its ground state, interacting with a linearly polarized laser pulse. We used an accurate spectral method to solve the TDSE in the dipole approximation and within the velocity gauge. In the configuration space, the TDSE is

$$\mathrm{i}\frac{\partial}{\partial t}\Phi(\mathbf{r},t) = \left[-\frac{\nabla^2}{2} - \frac{1}{r} - \mathrm{i}A(t)(\mathbf{e}\cdot\nabla)\right]\Phi(\mathbf{r},t), \tag{2}$$

where $\mathbf{e}$ is the unit polarization vector taken along the z-axis. $A(t)$ is the z-component of the vector potential given by

$$A(t) = A_0\cos^2\left[\frac{\pi t}{T}\right]\sin(\omega t + \phi), \qquad -\frac{T}{2} \le t \le \frac{T}{2}, \tag{3}$$

where ϕ is the carrier envelope phase and T, the full pulse duration. In terms of the peak intensity, the amplitude A_0 is given by

$$A_0 = \frac{1}{\omega}\sqrt{\frac{I}{I_0}}, \tag{4}$$

where $I_0 = 3.51 \times 10^{16}$ W/cm^2 is the atomic unit of intensity. Our spectral method consists in expanding the wave function $\Phi(\mathbf{r},t)$ in a basis composed of products of spherical harmonics $Y_{l,0}(\hat{r})$ and complex radial Coulomb sturmian functions $S^{\kappa}_{n,l}(r)$,

$$\Phi(\mathbf{r},t) = \sum_{n,l} a_{n,l}(t)\frac{S^{\kappa}_{n,l}(r)}{r}Y_{l,0}(\hat{r}), \tag{5}$$

where $a_{n,l}(t)$ are the time-dependent coefficients of the expansion. A detailed account of our spectral method is given in [14, 15]. We stress that a basis of Coulomb sturmian functions is particularly suited to describe accurately a large number of high-lying Rydberg states. The Coulomb sturmian functions are solutions of the radial field free Schrödinger equation for atomic hydrogen [16]. It means that by adjusting the nonlinear parameter κ to $1/n$, the

corresponding Coulomb sturmian function $S^{\kappa}_{n,l}(r)$ coincides with the exact radial wave function of the excited state of principal quantum number n and angular quantum number l. In fact the choice of κ allows one to monitor the region of the bound state spectrum and the number of bound states we want to describe accurately. In practice, we choose the value of the nonlinear parameter κ sufficiently small with a number of Coulomb sturmian functions per angular momentum relatively high, to be able to describe very accurately a large number of excited states. In the present calculations, we take $\kappa = 0.3$ and 2000 basis functions per angular momentum to represent accurately atomic states up to more than $n = 100$ for each value of the angular momentum. Describing such high lying excited states with a grid based method is prohibitively difficult since the size of the box needed would be extremely large. To treat the ionized part of the wave function, we use a complex value of the nonlinear parameter κ. This is equivalent to a global complex rotation of the full Hamiltonian. By choosing κ in the lower right quadrant of the complex plane, our wave function satisfies the physical boundary conditions of the problem, both in the closed and in the outgoing-wave open channels [14]. Contrary to our previous calculations [15], we time propagate the full wave function by means of the well-known Crank-Nicholson algorithm.

We also use the same spectral expansion to evaluate the probability of ionization in the adiabatic limit as given by Eq. (1). The width of the ground state as a function of the field is obtained by diagonalizing the complex rotated static field Stark Hamiltonian [17].

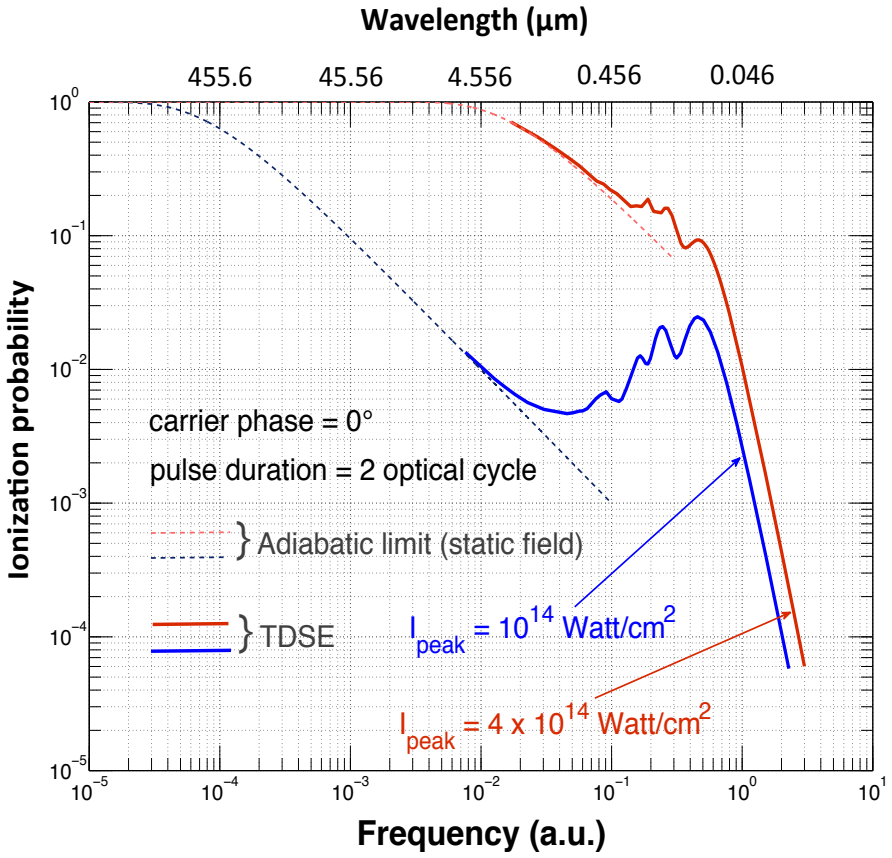

FIGURE 1. (Color online) Ionization yield as a function of frequency for the interaction of atomic hydrogen with a two optical cycle cosine squared pulse. Two peak intensities are considered : 10^{14} W/cm^2 (blue lines) and 4×10^{14} W/cm^2 (red lines). The solid lines have been obtained by solving numerically the TDSE. The broken lines correspond to the adiabatic limit given by Eq. (1).

To illustrate the onset of the different ionization regimes, we show in Fig. (1) the ionization yield as a function of frequency for the interaction of atomic hydrogen with a two optical cycle cosine squared pulse. We consider two peak intensities, $\mathrm{I_{peak}} = 10^{14}$ W/cm^2 and $\mathrm{I_{peak}} = 4 \times 10^{14}$ W/cm^2 and compare the results obtained by solving the TDSE with the ones given in the adiabatic limit by Eq. (1). For frequencies above the ionization potential ($\omega > 0.5$), both

curves exhibit a smooth behavior as predicted in the lowest order of perturbation theory. The frequency for which the adiabatic limit is reached depends on the pulse peak intensity. For $I_{peak} = 10^{14}$ W/cm^2, this limit is reached for $\omega = 0.01$, which corresponds to a wavelength $\lambda = 4.5\ \mu m$ and the adiabaticity parameter $\gamma = 0.19$. For $I_{peak} = 4\times10^{14}$ W/cm^2, the adiabatic limit is reached for $\omega = 0.07$, which corresponds to $\lambda = 651$ nm and $\gamma = 0.66$. Between these two limits, we find an intermediate regime in which both yields show modulations which result from the presence of closing channel thresholds. For the lower peak intensity, the ionization yield shows a "zigzag" behavior which results from the interplay between tunneling and multiphoton processes [18]). This "zigzag" behavior and the broad minimum seen around $\lambda = 800$ nm (which corresponds to $\gamma = 1$) is not present for the higher peak intensity. In fact, at this peak intensity and $\lambda = 800$ nm, the ground state is over the potential barrier.

III. RESULTS

Our aim is to elucidate the mechanism leading to the excitation of many Rydberg states in the adiabatic and non-adiabatic tunneling regimes. Explicitly, we do not perform a focal averaging of the calculated excitation probability since that won't alter but may obscure such mechanisms. We first consider the interaction of atomic hydrogen with a 40-cycle pulse of 800 nm wavelength. The pulse has a 2-cycle sine squared turn on and off with 36 cycles on

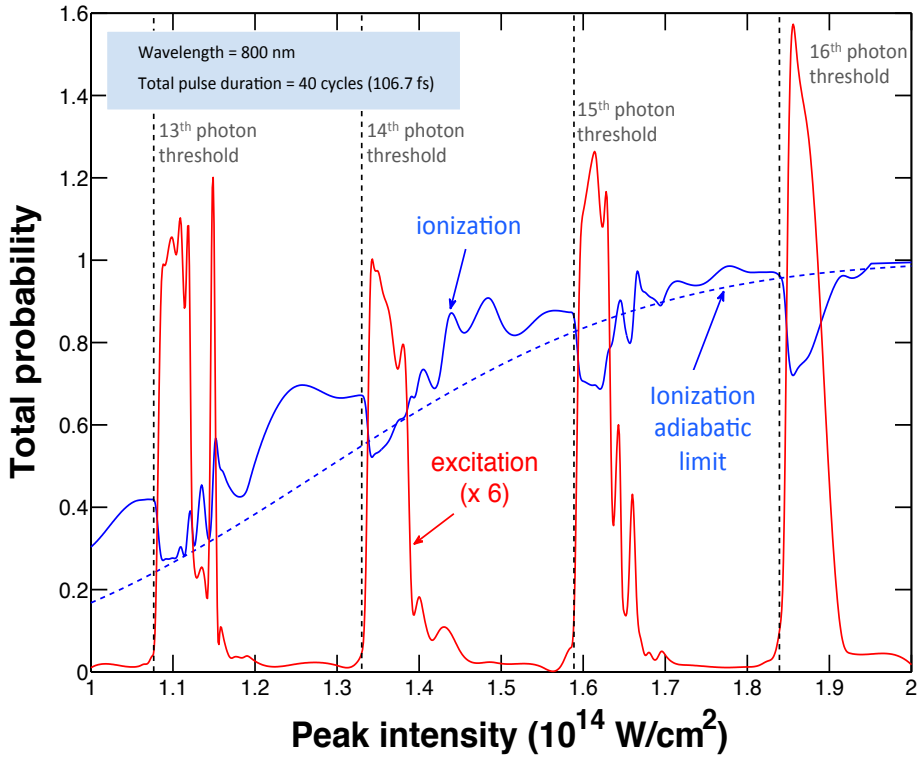

FIGURE 2. (Color online) Probability of ionization (solid blue curve) and excitation (red curve) of atomic hydrogen exposed to a 40-cycle pulse of 800 nm wavelength as a function of the peak intensity, evaluated by solving the TDSE. The pulse has a 2-cycle sine squared turn on and off has a total duration of 40 cycles. The dashed blue curve shows the probability of ionization in the adiabatic limit as given by Eq. (1). The vertical dashed lines indicate the position of the successive Nth-photon thresholds.

the flat-top giving a total duration of 40 cycles (106 fs) as opposed to the pulse shape defined in Eq. (3). Fig. (2) shows the probability of excitation and ionization obtained by solving the TDSE as a function of the peak intensity. For comparison, we also show the probability of ionization in the adiabatic limit. The behavior of the ionization probability is very similar to the behavior of the ionization rate evaluated within Floquet theory [19, 20] with one striking difference. According to Floquet theory, the ionization potential and therefore the number of photons required to ionize the atom increases with peak intensity due to the AC-Stark shift of the atomic levels. Between any pair of successive N-photon thresholds (indicated by vertical dashed lines in Fig. (1)), the behavior of the ionization

probability is qualitatively similar : a smooth region followed by a region of isolated (Freeman type) resonances and a broad hilly structure. However, in [19, 20], it was shown that the behavior of the ionization rate is nearly constant just below and above each N-photon threshold. This contrasts with the behavior of the ionization probability shown in Fig. (2), where the ionization probability is indeed flat below each N-photon threshold but surprisingly exhibits a very sharp drop just above each threshold before becoming flat again. It is precisely just above each N-photon threshold that the probability of excitation (the red curve in Fig. (2)) shows a significant increase. Let us note that for the frequencies and intensities considered in [19, 20] and in the present work, Floquet calculations are prohibitively difficult and must rely on some approximations. In Fig. (2), the dashed blue line shows the ionization probability as a function of the peak intensity in the adiabatic limit. Clearly, below the 15^{th} threshold, this limit is not yet reached and we are still in the non adiabatic tunneling regime ($\gamma \sim 1$).

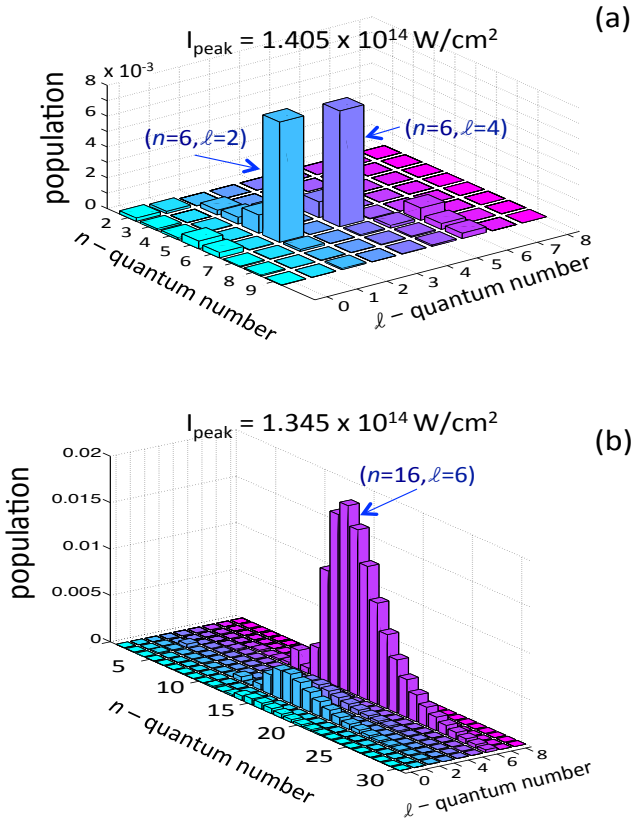

FIGURE 3. (Color online) Bar chart of the excited state population resulting from the interaction of atomic hydrogen with the same pulse as in Fig. (2). Populations are given as a function of n, the principal quantum number and ℓ, the angular quantum number for two values of the peak intensity just above the 14^{th} threshold : (a) $\text{I}_{\text{peak}} = 1.405 \times 10^{14}$ W/cm^2 and (b) $\text{I}_{\text{peak}} = 1.345 \times 10^{14}$ W/cm^2.

Let us now analyze the n and ℓ distribution of the excited states produced for the same pulse as in Fig. (2). We choose three values of the peak intensity between the 14^{th} and the 15^{th} photon threshold, approaching the 14^{th} threshold. In Fig. (3a), we consider a peak intensity $\text{I}_{\text{peak}} = 1.405 \times 10^{14}$ W/cm^2 in a region where isolated Freeman type resonances are seen in the ionization probability. In this case, population is found mainly in the $(n = 6, \ell = 2)$ and $(n = 6, \ell = 4)$ excited states. The fact that the angular momentum of the populated excited states has the same parity as N-1 where N is the minimum number of photons needed to ionize, is a consequence of selection rules within Floquet theory [20]. In Fig. (3b), we get closer to the 14^{th} photon threshold by choosing $\text{I}_{\text{peak}} = 1.345 \times 10^{14}$ W/cm^2. We see that a larger number of excited states with larger values of the principal quantum number n get populated, reaching values of n around 30. After the absorption of 14 photons, the atomic hydrogen is found in a region of the spectrum just below the ionization threshold where many Rydberg states are accessible. Contrary to Floquet theory where the field is monochromatic, we get a bunch of populated excited states from the pulse bandwidth. Like

in the previous case, only states with an even value of the angular momentum get populated. Furthermore, most

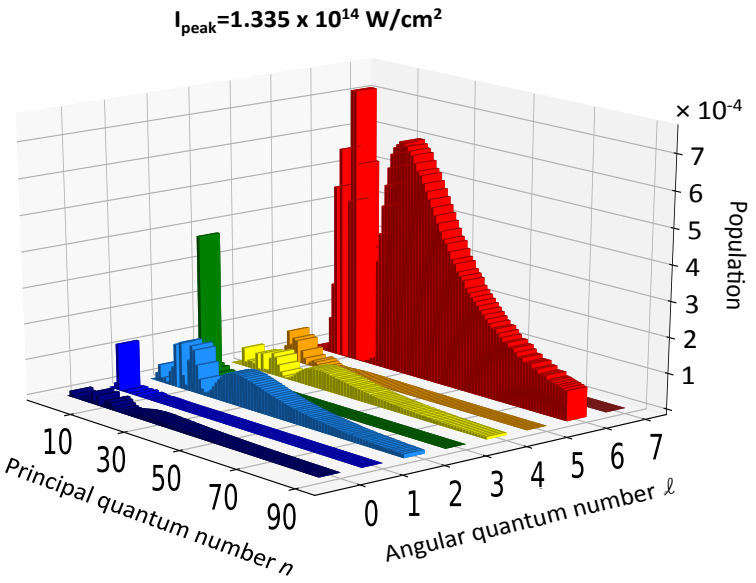

FIGURE 4. (Color online) Bar chart of the excited state population resulting from the interaction of atomic hydrogen with the same pulse as in Fig. (2). Populations are given as a function of n, the principal quantum number and ℓ, the angular quantum number for $I_{peak} = 1.335 \times 10^{14}$ W/cm^2, an intensity just above but almost at the 14^{th} threshold.

of the Rydberg states which are populated have an angular quantum number $\ell = 6$. This value is the highest one for which excited states are populated. This result agrees with the semiclassical estimation of $\ell_{max} = \sqrt{A_0/\omega^3}$ [21]. Fig. (4) shows the distribution of (n, ℓ) excited states for $I_{peak} = 1.335 \times 10^{14}$ W/cm^2 which is right above the 14^{th} photon threshold. In this case, we explore the region of the high-lying Rydberg states, just below threshold. We see that excited states with principal quantum numbers n close to 100 and beyond are then populated. As in Fig. (3), the highest angular momentum of the populated excited states is again 6, confirming the semiclassical estimation. According to Floquet theory, resonant transitions via intermediate Rydberg states of large angular momentum ℓ are strongly suppressed [20] for lower peak intensities. Note that a small fraction of low lying excited states with odd value of ℓ are populated because of the turn on and off of the pulse. We have checked that for higher peak intensities beyond the 16^{th} photon threshold where the ionization probability tends to its adiabatic limit, the trapping of population in excited states shows similar features. In addition, we have checked the dependence of our results on the turn on and turn off by repeating the calculations shown in Figs (2)-(4) for a 4 cycle turn on and turn off and we found no qualitative difference in the distributions shown.

Our findings for long pulses show the multiphoton character of the excitation process taking place. This explains clearly why the trapping of population is very sensitive to the value of the peak intensity. For some peak intensities just above each N-photon threshold, many Rydberg states are populated while below, no trapping is observed. In addition, the populated excited states have an angular momentum with a well defined parity, fixed by the minimum number of photons needed to ionize. This in turn depends on the peak intensity used. We now proceed by considering shorter pulses of the form given in Eq. (3).

In Fig. (5), we consider a cosine squared pulse of 10 optical cycles (27fs) and a range of peak intensities from 3.5×10^{14} W/cm^2 to 5×10^{14} W/cm^2, which corresponds to a value of the adiabaticity parameter γ around 0.5. We show the probability of ionization and excitation calculated by solving the TDSE as well as the probability of ionization evaluated in the adiabatic limit (from Eq. (1)) as a function of the peak intensity. We first note that the ionization probability closely follows its adiabatic limit except when the excitation probability becomes significant. The latter exhibits clear out-of-phase oscillations with respect to the ionization probability as observed by Li *et al.*

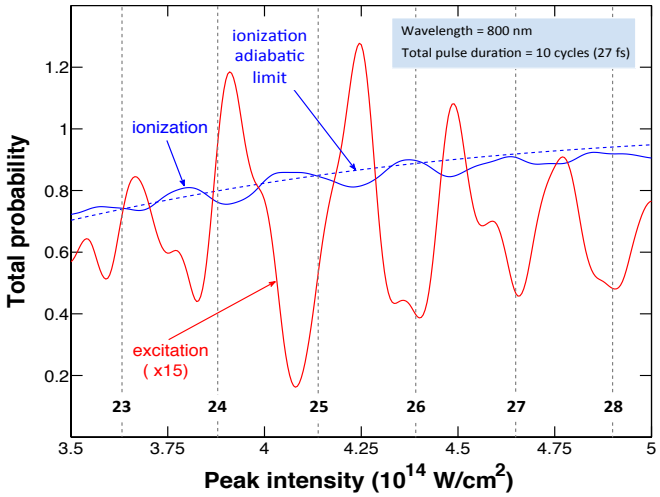

FIGURE 5. (Color online) Total probability of ionization (solid blue curve) and excitation (red curve) of atomic hydrogen exposed to a 10-cycle cosine squared pulse of 800 nm wavelength as a function of the peak intensity, evaluated by solving the TDSE. The dashed blue curve shows the total probability of ionization in the adiabatic limit as given by Eq. (1). The vertical dashed lines indicate the position of the successive N$^{\rm th}$-photon thresholds with N given by the number at the bottom of each vertical line.

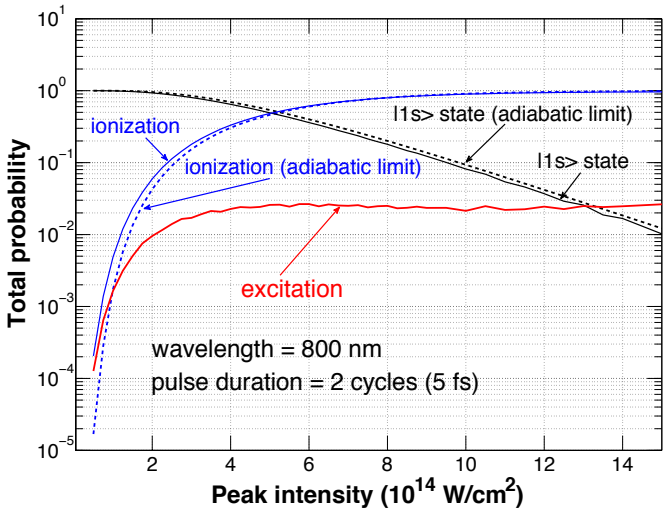

FIGURE 6. (Color online) Total probability of ionization (blue lines), excitation (red line) and to stay in the ground state (black lines) for atomic hydrogen exposed to a 2-cycle cosine squared pulse of 800 nm wavelength as a function of the peak intensity. The solid lines are obtained by solving the TDSE and the dashed lines give the adiabatic limit (from Eq. (1)).

[9, 10] but for lower peak intensities. These oscillations are punctuated by the presence of the N-photon thresholds, which is compatible with a multiphotonic view of the excitation mechanism.

The modulation of the ionization probability punctuated by the presence of the N-photon thresholds is reproduced within the strong field approximation (SFA). This is due to the fact that, within the SFA, the outgoing electrons are described by Volkov states that take correctly into account the ponderomotive shift of the ionization threshold. As stressed in [11], the decrease of the ionization probability for peak intensities just above each N-photon threshold results from an intra-cycle interference between electron wave packets emitted at two consecutive maxima of the electric field. In other words, the modulations present in the ionization probability can be viewed as the consequence of either a multiphoton process or an interference effect. However, within the leading order SFA, the recapture of an ejected electron into any excited state is not described. This point has been discussed in detail in [22] where a

generalized SFA treatment inspired by the Faddeev formalism of scattering theory has been introduced.

In Fig. (6), we consider the interaction of an ultrashort cosine squared laser pulse of 2-cycle full duration (5fs) and 800 nm wavelength with atomic hydrogen. We show the excitation probability as well as the probability to stay in the ground state and the ionization probability for a wide range of peak intensities from 10^{14} W/cm^2 to 1.5×10^{15} W/cm^2. We also show the ionization probability and the probability to stay in the ground state evaluated in the adiabatic limit (Eq. (1)). At low peak intensities, the probability of excitation keeps increasing with the peak intensity until it reaches 4×10^{14} W/cm^2. Beyond this value, the probability of excitation becomes practically constant despite small modulations. This strong increase of the excitation probability is also present in [10] and has been recently emphasized in [11] both experimentally and theoretically. We analyzed in detail the ℓ and n distributions of the excited state population for peak intensities where the probability of excitation is constant. We found that both distributions are peaked around rather small values (3 or 4) of the quantum numbers n and ℓ, even for very high peak intensities. However once the peak intensities get large, these n and ℓ distributions exhibit a long tail. Electrons in excited states with high ℓ and n are most of the time located far away from the nucleus where the effective interaction of the electron with the external field is weak. Such an electron is quasi free and therefore cannot absorb or emit photons. This explains why the probability of excitation becomes constant for high peak intensities. However, atoms in relatively low-lying ($n = 3$ or 4) excited states do also survive the high peak intensities. In this case, the survival of these low-lying states can be explained by a destructive interference process as described in [23–25]. Finally, it is interesting to see that, at high peak intensities, the probability of ionization and to stay in the ground state obtained by solving the TDSE tend smoothly to their adiabatic limit.

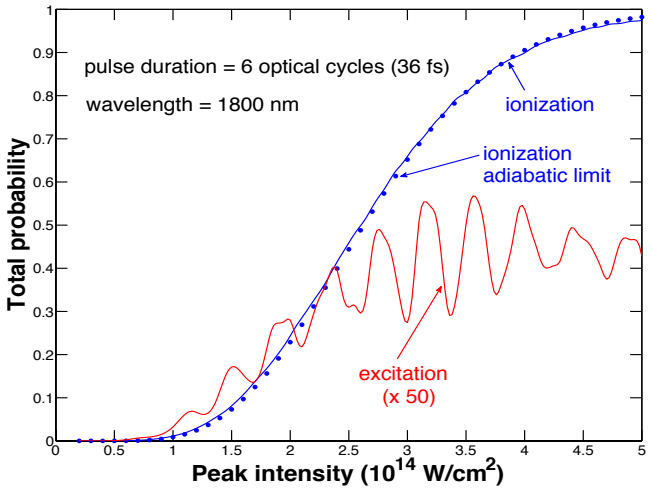

FIGURE 7. (Color online) Total probability of ionization (solid blue curve) and excitation (red curve) of atomic hydrogen exposed to a 6-cycle cosine squared pulse of 1800 nm wavelength as a function of the peak intensity, evaluated by solving the TDSE. The blue dots show the total probability of ionization in the adiabatic limit as given by Eq. (1).

In all the cases discussed above, the amplitude of the quiver motion of the electron remains always less than 60 a.u. This is much smaller than the spatial extent of the high lying excited states, which are populated during the interaction. By contrast, we are now going to consider quiver motion amplitudes up to 200 a.u. and the quasi-static limit. In Fig. (7), we consider the interaction of atomic hydrogen with a 6-cycle cosine squared pulse of λ =1800 nm wavelength ($\omega = 0.025$ a.u.) (36fs) for peak intensities ranging from 0 to 5×10^{14} W/cm^2. Results are shown for the probability of ionization and excitation, obtained by solving the TDSE. Converged results are obtained for the highest intensity with 2000 sturmians and $l_{max} = 191$. We also show the probability of ionization in the adiabatic limit as given by Eq. (1). At this wavelength, the results for the ionization probability obtained both by solving the TDSE and by using Eq. (1) are in perfect agreement over the whole range of peak intensities. This shows that for λ =1800 nm, we are clearly in the quasi static tunneling regime. In addition, the amount of population trapped in excited states is much smaller than for shorter wavelengths. We have checked that decreasing the field frequency leads to a systematic reduction of the excitation probability. However in the tunneling model of Landsman *et al.* [26] it is expected that the excitation probability should be proportional to the tunneling probability which means that the excitation probability would be expected to increase for increasing wavelengths (see Fig. 1). While examining the

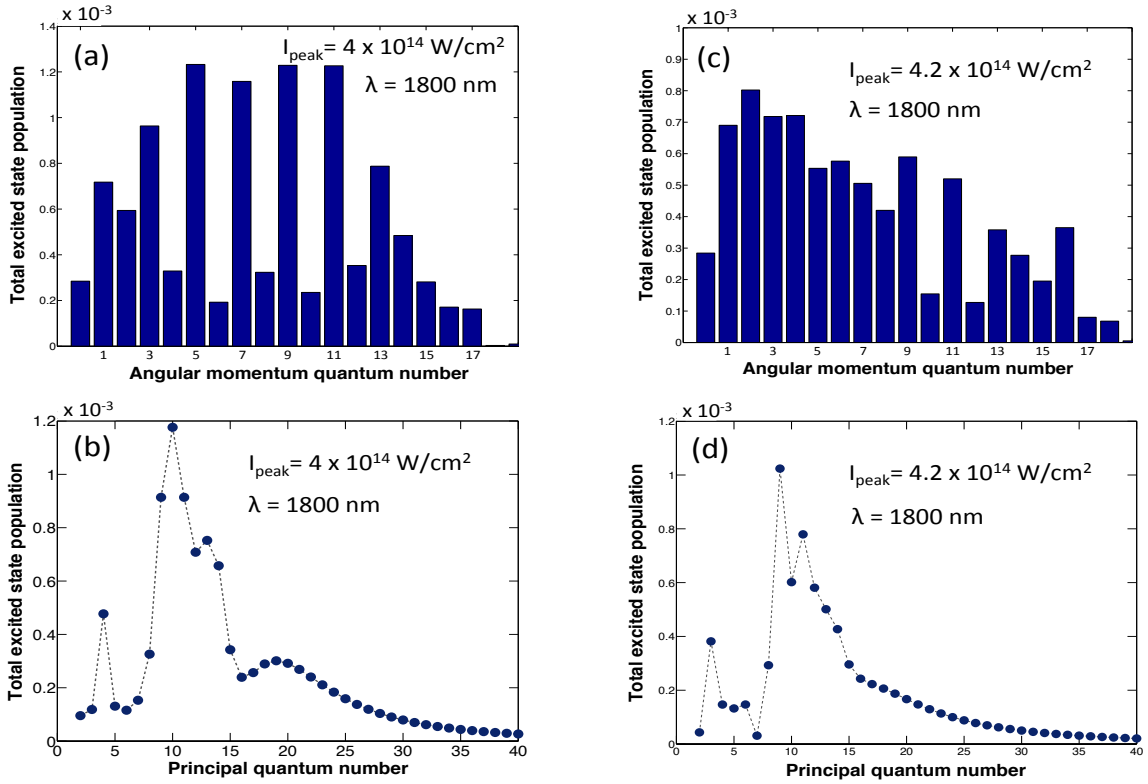

FIGURE 8. (Color online) Excited state population resulting from the interaction of atomic hydrogen with the same pulse as in Fig. (7). These populations are given as a function of the angular momentum quantum number for (a) $I_{peak} = 4 \times 10^{14}$ W/cm^2 and (c) $I_{peak} = 4.2 \times 10^{14}$ W/cm^2. In (b) and (d), these populations are shown a function of the principal quantum number for the same peak intensities, respectively.

physical mechanism that determines whether a tunneled electron will be recaptured into the ground state thereby leading to high order harmonic generation (HOHG) or be captured in a Rydberg state, Landsman *et al.* [26] noted that HOHG will be efficient only if the electron returns very close to the parent ion. This constraint does not exist in the case of recombination into an excited state. We also see in Fig. (7) that the excitation probability exhibits oscillations that are more regular than those observed before. However, now, they are no longer punctuated by the presence of the N-photon thresholds. Indeed, calculating the AC-Stark shift in second order, we would get several hundred thresholds in the range of peak intensities we show. At the peak intensity of 5×10^{14} W/cm^2, we have a ponderomotive energy U_p of 150 eV so that about 218 photons are necessary to ionize the atom in its ground state. Finally, a close look at the ionization probability curve shows small modulations that are in phase opposition to the excitation probability oscillations. In this case, the modulations of the ionization probability can no longer be described within the SFA.

To gain more insight on the nature of the oscillations in the excitation probability, we consider in Fig. (8) the n and ℓ distributions of the excited state populations for two values of the peak intensity, $I_{peak} = 4 \times 10^{14}$ W/cm^2 and $I_{peak} = 4.2 \times 10^{14}$ W/cm^2, corresponding respectively to a maximum and a minimum of the excitation probability shown in Fig. (7). The distributions for any other two adjoining maxima and minima in Fig. (8) exhibit the same qualitative behavior as we are about to describe. Besides a migration of the excited state population towards higher values of ℓ in both cases, the shape of the ℓ distribution of the excited state population differs significantly between the maxima and minima. In the case of a minimum, there is a slow decrease of the ℓ distribution with increasing ℓ while for a maximum, we observe a gaussian shape with the dominant values of ℓ having a well defined parity. The mechanisms behind these new features are still unclear but we propose the following tentative explanation. At the maximum we attribute this last feature of the ℓ distribution to resonant Raman transitions via the continuum coupling Rydberg states of the same n and different ℓ [27]. This could explain the observed migration to states of higher ℓ as well as

the stability of high ℓ states with respect to ionization. In addition, the distribution in n (Fig. (8b)) is compatible with the ℓ distribution (Fig. (8a)). Indeed, for a given value of n, the maximum value of ℓ reached through resonant Raman coupling must satisfy $\ell = n - 1$. In Fig. (8b), the dominant values of n are below $n = 15$ and the dominant values of ℓ shown in Fig. (8a) are below $\ell = 14$. The reason for the behavior of the ℓ distribution at a minimum of the excitation probability is not clear. In any case, the migration from an (n, ℓ) state towards n-states of larger value of ℓ starts once the Raman Rabi frequency becomes larger than the ionization rate from this (n, ℓ) state. Since both the ionization rate and the Rabi frequency for the resonant Raman process are proportional to the intensity, it means that there is a threshold peak intensity for which the migration starts [27, 28]. On the other hand, since the laser frequency is much higher than the natural frequency of the high-lying excited states, we expect the ionization rate from these excited states to be rather small and therefore the threshold peak intensity to be rather low. In the present case, the migration is already present below 10^{14} W/cm^2. For the whole range of peak intensities considered here, we have checked that the highest value of ℓ for which states are populated follows again the semiclassical estimate.

IV. TIME-EVOLUTION OF THE EXCITED WAVE PACKET

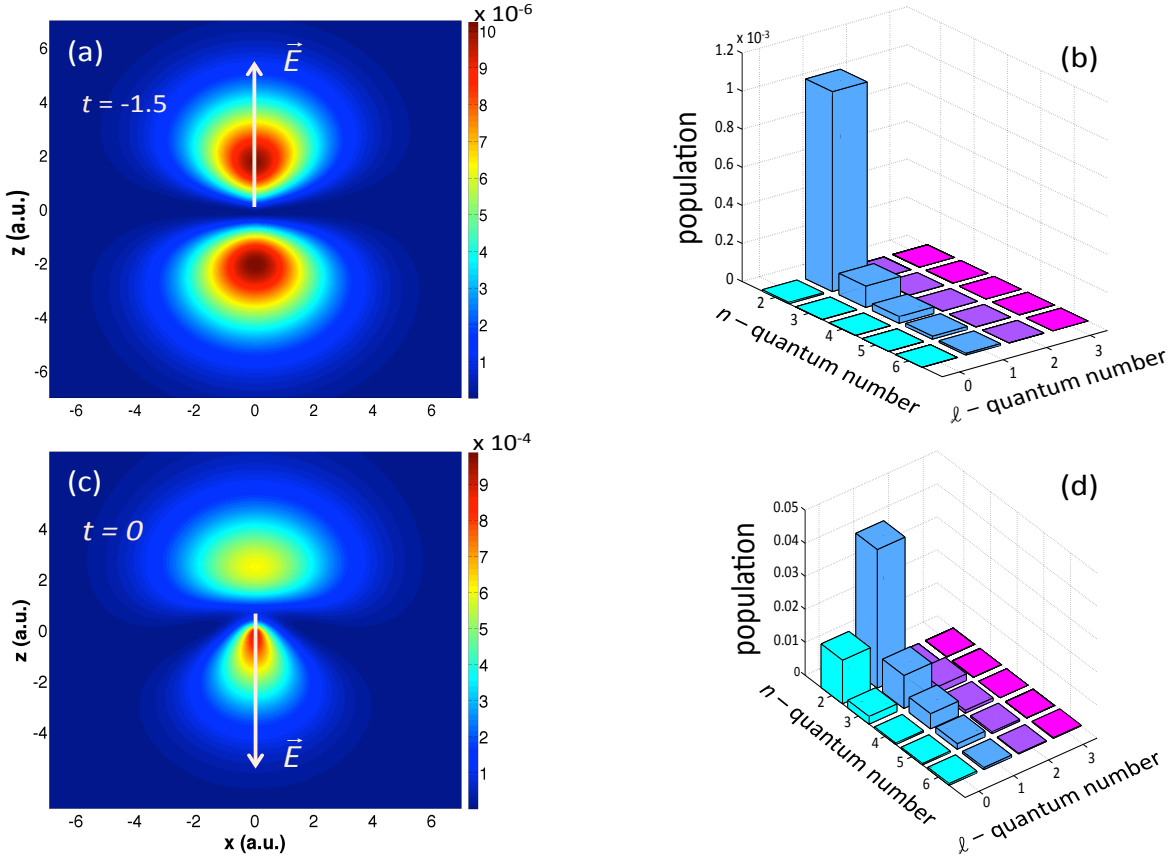

FIGURE 9. (Color online) Time evolution of the excited wave packet resulting from the interaction of atomic hydrogen with a 4-cycle cosine squared pulse of 800 nm wavelength and 4×10^{14} W/cm^2 peak intensity. The left panels show a plot of the modulus squared of this wave packet in the x-z plane at two times during the interaction with the pulse : (a) $t = -1.5$ optical cycles and (b) $t = 0$ (middle of the pulse) for which the vector potential is zero. The arrow indicates the electric field vector. The right panels (b) and (d) give the corresponding n and ℓ distribution of the populations.

Finally to try to lend further insight into the process of excitation and ionization we plot how the excited state wave packet builds up during the interaction with the radiation pulse and obtain the (n, ℓ) distribution at particular times during the pulse. We consider a 4-cycle cosine squared pulse of 800 nm wavelength and $4{\times}10^{14}$ W/cm^2 peak intensity. We calculate the excited state wave packet at times t for which the vector potential is identically zero so

that the results are gauge independent. At these times, the adiabatic Stark basis coincides with the atomic basis. In Fig. (9), we show the modulus squared of the excited state wave packet in the x-z plane as well as the (n, ℓ) distribution of population for two times : $t = -1.5$ optical cycles at the beginning of the pulse and $t = 0$ at the middle of the pulse. At $t = -1.5$ optical cycles, we observe that an excited state wave packet has been created with an up-hill component parallel to the electric field and a down-hill component opposite to the field. We also see from the (n, ℓ) distributions that only p-states, in particular the 2p and 3p states, are populated. These p-states represent the polarization of the atomic cloud by the field. In the middle of the pulse at $t = 0$ where the electric field is maximum, the down-hill component of the excited state wave packet is more diffuse, as expected, since we are now in the over-the-barrier regime. By contrast, the up-hill component shows a strong localization very close to the nucleus because of the potential barrier. At this time, we see a significant increase of the p-state population. In addition, the electric field mixes degenerate s and p as well as p and d states.

In Fig. (10), we consider the time evolution of the excited wave packet towards the end of the radiation pulse. At $t = 1.5$ optical cycles, the excited state wave packet has spread at large distances on both sides of the nucleus. However there is still an important localization of the excited state wave packet on the up-hill side. Together with the spreading of the wave packet, we note that more levels of higher ℓ and n are populated. At the end of the radiation pulse at $t = 2$ optical cycles, a strong localization of the excited state wave packet persists close to the nucleus while the remaining part of this wave packet keeps spreading away from the nucleus. In panel (d), we see that the states of principal quantum number $n = 5, 6$ and 7 are predominantly populated. In addition, states of odd ℓ are the most important.

Whilst these snapshots in time provide a picture of how the wave packet evolves and the (n, ℓ) distribution at particular

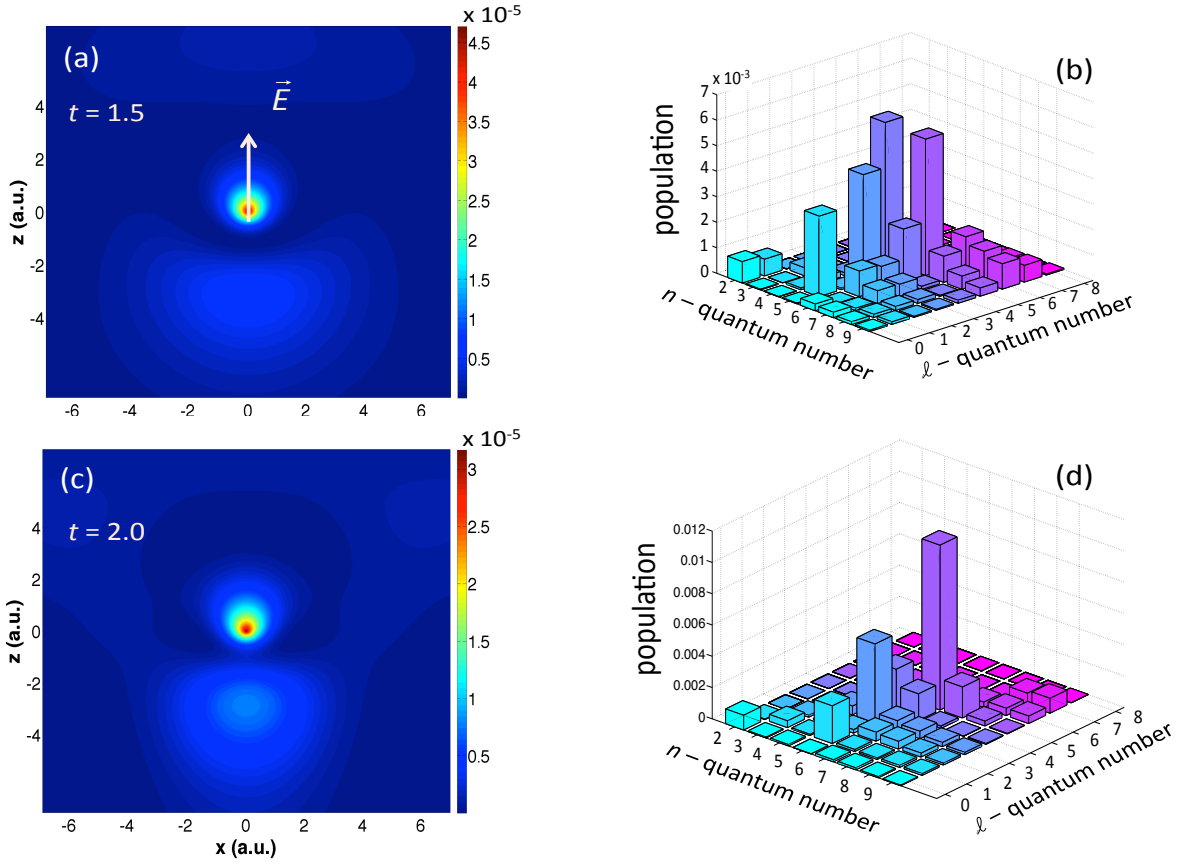

FIGURE 10. (Color online) Time evolution of the excited wave packet resulting from the interaction of atomic hydrogen with a 4-cycle cosine squared pulse of 800 nm wavelength and 4×10^{14} W/cm^2 peak intensity. The left panels show a plot of the modulus squared of this wave packet in the x-z plane at two times during the interaction with the pulse : (a) $t = 1.5$ optical cycles and (b) $t = 2$ optical cycles (end of the pulse) for which the vector potential is zero. The arrow indicates the electric field vector. The right panels (b) and (d) give the corresponding n and ℓ distribution of the populations.

times during the pulse it is not straightforward to relate the evolution of the wave packet to either mechanism, frustrated tunneling or multiphoton excitation.

V. CONCLUSION AND PERSPECTIVE

In conclusion, we have studied the strong field excitation of Rydberg states in atomic hydrogen in both the quasi static and non adiabatic tunneling regimes. To perform this study, we used a spectral method based on complex sturmian functions, that are known to describe very accurately the hydrogen bound spectrum, to solve the TDSE. In addition, we use the same sturmian basis to obtain the ionization probability in the quasi static field limit by calculating the ground state width as a function of the instantaneous static field. We have studied probabilities of excitation and ionization as a function of the peak intensity for various pulse durations and two wavelengths, 800 nm and 1800 nm.

At 800 nm for a very long pulse of 40 cycles duration, we have shown that the trapping of population in high-lying Rydberg states, of principal quantum number $n \approx 100$, is extremely sensitive to the value of the peak intensity. In fact, due to the AC-Stark effect, this trapping of population occurs only for peak intensities just above each N-photon threshold. This result disagrees with previous investigations based on Floquet theory. Furthermore, most of the populated high-lying Rydberg states have the same value of the angular momentum quantum number. This value, which agrees very well with the semiclassical estimate of the maximum value of the angular momentum, has a well defined parity equal to the parity of the number of photons needed to reach these high-lying Rydberg states. All these features, which occur in the non adiabatic tunneling regime where the amplitude of the electron quiver motion is much smaller than the spatial extent of the populated Rydberg states, are compatible with multiphotonic excitation. For shorter pulse durations, we considered higher peak intensities thereby entering in the quasi-static tunneling regime. In this case, these features persist but are less pronounced. In particular, the probability of excitation keeps oscillating as a function of intensity in phase opposition to the ionization probability and with a frequency determined by the presence of the N-photon thresholds. For ultrashort pulses, these oscillations are strongly damped but, as before, the excitation probability increases rapidly with the peak intensity until it reaches a value around 4×10^{14} W/cm^2 beyond which it becomes constant as a result of the stability of the populated excited states against ionization.

At 1800 nm, for the range of peak intensities we considered, we are deep in the quasi-static tunneling regime. The excitation probability shows very regular oscillations as a function of the intensity again in phase opposition with the ionization probability. However, the frequency of these oscillations can no longer be explained in terms of the second order AC-Stark shift of the atomic levels. The analysis of the n and ℓ distributions of the Rydberg state population shows a migration of population towards higher angular momenta, the maximum value of which agrees very well with the semiclassical estimate. The distribution in ℓ at each maximum of the excitation probability is tentatively explained as being due to resonant Raman transitions via the continuum coupling Rydberg states of the same n and different ℓ. However, at each minimum of the excitation probability, the behavior of the ℓ distribution is not yet fully understood thereby requiring further investigation. We also observed that for higher wavelengths, the probability of excitation decreases systematically.

In order to analyze the trapping of Rydberg states from a time dependent perspective, we calculated and represented the modulus squared of the excited state wave packet, during the interaction with the pulse at times t for which the vector potential is zero and hence gauge invariant. We also calculated the (n, ℓ) distribution at these times and showed how it evolves during the pulse.

VI. ACKNOWLEDGEMENTS

A.G. is "aspirant au Fonds de la Recherche Scientifique (F.R.S-FNRS)". Y.P. thanks the Université Catholique de Louvain (UCL) for financially supporting several stays at the Institute of Condensed Matter and Nanosciences of the UCL. F.M.F and P.F.O'M gratefully acknowledge the European network COST (Cooperation in Science and Technology) through the Action CM1204 "XUV/X-ray light and fast ions for ultrafast chemistry" (XLIC) for financing several short term scientific missions at UCL. The present research benefited from computational resources made available on the Tier-1 supercomputer of the Fédération Wallonie-Bruxelles funded by the Région Wallonne under the grant n^{o}1117545 as well as on the supercomputer Lomonosov from Moscow State University and on the supercomputing facilities of the UCL and the Consortium des Equipements de Calcul Intensif (CECI) en Fédération Wallonie-Bruxelles funded by the F.R.S.-FNRS under the convention 2.5020.11. Y.P. is grateful to Russian Foundation for Basic Research (RFBR) for the financial support under the grant N16-02-00049-a.

[1] L.V. Keldysh, Sov. Phys. JETP **20**, 1307 (1965).
[2] F.Krausz and M.Ivanov, Rev. Mod. Phys. **81**, 163 (2009).
[3] T. Nubbemeyer, K. Gorling, A. Saenz, U. Eichmann and W. Sandner, Phys. Rev. Lett. **101**, 233001 (2008).
[4] S. Larimian, S. Erattupuzha, Ch. Lemell, S. Yoshida, S. Nagele, R. Maurer, A. Baltuska, J. Burgdörfer, M. Kitzler and X. Xie, Phys. Rev. A **94**, 033401 (2016).
[5] R.R. Jones, D.W. Schumacher and P.H. Bucksbaum, Phys. Rev. A **47**, R49 (1993).
[6] E.S. Toma, Ph. Antoine, A. de Bohan and H.G. Muller, J. Phys. B **32**, 5843 (1999).
[7] M. Chini, X. Wang, Y. Cheng, H. Wang, E. Cunningham, P.-C. Li, J. Heslar, D.A. Telnov, S.-I. Chu and Z. Chang, Nature Photonics **8**, 437 (2014).
[8] S. Beaulieu, S. Camp, D. Descamps, A. Comby, V. Wanie, S. Petit, F. Légaré, K.J. Schafer, M.B. Gaarde, F. Catoire, and Y. Mairesse, Phys. Rev. Lett. **117**, 203001 (2016).
[9] Q. Li, X.-M. Tong, T. Morishita, H. Wei and C.D. Lin, Phys. Rev. A **89**, 023421 (2014).
[10] Q. Li, X.-M. Tong, T. Morishita, C. Jin, H. Wei and C.D. Lin, J. Phys. B **47**, 204019 (2014).
[11] H. Zimmermann, S. Patchkovskii, M. Ivanov, and U. Eichmann, Phys. Rev. Lett. **118**, 013003 (2017).
[12] H. Liu, Y. Liu, L. Fu, G. Xin, D. Ye, J. Liu, X.T. He, Y. Yang, X. Liu, Y. Deng, C. Wu, and Q. Gong, Phys. Rev. Lett. **109**, 093001 (2012).
[13] G.L.Yudin and M.Y. Ivanov, Phys. Rev. A **64**, 013409 (2001).
[14] B. Piraux and R. Shakeshaft, Phys. Rev. A **49**, 3903 (1994).
[15] E. Huens, B. Piraux, A. Bugacov and M. Gajda, Phys. Rev. A **55**, 2132 (1997).
[16] J. Avery, Generalized Sturmians and Atomic Spectra, World Scientific, Singapore, (2006).
[17] I.W. Herbst and B. Simon, Phys. Rev. Lett. **41**, 67 (1978).
[18] D. Dimitrovski and E A Soloviev, J. Phys. B **39**, 895 (2006).
[19] R. M. Potvliege and R. Shakeshaft, Phys. Rev. A **40**, 3061 (1989).
[20] K. Krajewska, I.I. Fabrikant and A. Starace, Phys. Rev. A **86**, 053410 (2012).
[21] D. G. Arbo, K. I. Dimitriou, E. Persson, and J. Burgdörfer, Phys. Rev. A **78**, 013406 (2008).
[22] Y. V. Popov, A. Galstyan, F. Mota-Furtado, P.F. O'Mahony and B. Piraux, European Physical Journal D, **71**, 93 (2017).
[23] M.V. Fedorov and A.M. Movsesian, J. Opt. Soc. Am. B **6**, 928 (1989) ; J. Opt. Soc. Am. B **6**, 1504 (1989).
[24] M.V. Fedorov and M.Yu. Ivanov, J. Opt. Soc. Am. B **7**, 569 (1990).
[25] J. Parker and C.R. Stroud Jr., Phys. Rev. A **41**,1602 (1990).
[26] A. S. Landsman, A. N. Pfeiffer, C. Hofmann, M. Smolarski, C. Cirelli and U. Keller, New Journal of Physics **15**, 013001 (2013).
[27] J.D. Corless and C.R. Stroud Jr., Phys. Rev. Lett. **79**, 637 (1997).
[28] R. Grobe, G. Leuchs and K. Rzazewski, Phys. Rev. A **34**, 1188 (1986).